2021 Fifth IEEE International Conference on Robotic Computing (IRC) | 978-1-6654-3416-4/21/$31.00 ©2021 IEEE | DOI: 10.1109/IRC52146.2021.00010

Vibration Control for Pivoting by Robot Hand Equipped with CAVS and FingerVision

Yoshiyuki Suzuki
Graduate School of Information Sciences
Tohoku University
Sendai, Japan
Email: yoshiyuki.suzuki.s2@dc.tohoku.ac.jp

Akihiko Yamaguchi
Graduate School of Information Sciences
Tohoku University
Sendai, Japan
Email: info@akihikoy.net

Seita Nojiri
Graduate School of Natural Science & Technology
Kanazawa University
Kanazawa, Japan
Email: nose10118@stu.kanazawa-u.ac.jp

Tetsuyou Watanabe
Institute of Science and Engineering
Kanazawa University
Kanazawa, Japan
Email: twata@se.kanazawa-u.ac.jp

Koichi Hashimoto
Graduate School of Information Sciences
Tohoku University
Sendai, Japan
Email: koichi.hashimoto.a8@tohoku.ac.jp

***Abstract*—We explore in-hand manipulation, especially pivoting, with a robot hand equipped with a contact area variable surface (CAVS) and a vision-based tactile sensor FingerVision. CAVS is a skin for robots where the surface friction coefficient passively changes according to the external force; during holding objects with a small force, the friction coefficient is low, while the friction coefficient becomes higher when increasing the holding force. FingerVision provides multimodal sensations, including force and slip distributions, and orientation of grasped objects. On our robot hand, CAVS is embedded on the surface of the fingertips, and FingerVision is installed under the CAVS skin. With this hand, we expect a gentle in-hand manipulation of objects where we properly control objects by slipping them on purpose to achieve a desired operation, however an adequate control method for such operations has been unclear. This paper focuses on the control methods of the CAVS+FingerVision hand for pivoting objects as an example of in-hand manipulation. Through the empirical comparisons, we found that a vibration control of fingertips achieves the best accuracy and outperforms a simple fuzzy control, and CAVS outperforms a usual flat skin.**

***Index Terms*—robot hand, robotic manipulation, pivoting, vision-based tactile sensor, variable friction**

I. Introduction

In-hand manipulation is an important challenge of robotics since it improves the efficiency by operating objects without placing on the environment. An example is changing a posture of grasped objects such as a screwdriver; when a robot needs to change the posture of the screwdriver after grasping it, doing it within the hand will be faster than that with placing and re-grasping the driver. In such operations, sometimes it is useful to slip the grasped objects on purpose especially when the hand of the robot is simple like a parallel jaw gripper.

The surface of the robot hand matters when producing slippage on purpose; lower friction is better for a smooth slippage. On the other hand, higher friction is needed for holding objects stably. For solving this trade-off, we have been studying a robotic skin where we can control the friction coefficient of the surface. In a past study, we proposed a CAVS (contact area variable surface) mechanism as such a variable-friction surface [1]. CAVS consists of flexible protrusions; they deform according to the load on them, which changes

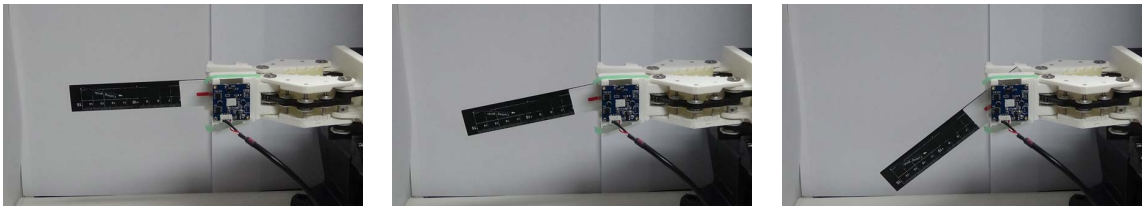

Fig. 1: Side view in pivoting

978-1-6654-3416-4/21/$31.00 ©2021 IEEE
DOI 10.1109/IRC52146.2021.00010

the contact area between the robot and the objects. CAVS is a passive mechanism whose surface friction coefficient changes as the contact area changes according to the external force. During holding objects with a small force, the friction coefficient is low, while the friction coefficient becomes higher when increasing the holding force. Because of its passivity and the simple structure, CAVS can be compact enough to embed on fingertips on robot hands, and it is easy to install tactile sensors under CAVS.

Meanwhile, in automating in-hand manipulation, sensing the current contact state between the hand and the objects would be beneficial. We introduce a vision-based tactile sensor FingerVision developed by our group [2]. FingerVision consists of a transparent elastic skin and a camera. It provides multimodal sensations, including force and slip distributions, and orientation of grasped objects. In this work, we replace the transparent elastic skin of FingerVision by the CAVS skin made with a transparent material in order to make a CAVS+FingerVision structure on a robot hand.

In this study, we have two research questions: (1) is a robot hand equipped with CAVS and FingerVision effective in in-hand manipulation? and (2) how can we properly control the robot hand equipped with CAVS and FingerVision in in-hand manipulation? In order to find answers to them, this paper uses pivoting of a 2-finger robot hand as an example task of in-hand manipulation. The pivoting task here is rotating an object around the grasped point by controlling slip with gravity and fingertip opening until it reaches to a target angle (cf. [3]). We solve this task with the 2-finger hand equipped CAVS and FingerVision; Fig. 1 shows a demonstration of pivoting with this system.

More concretely, this paper focuses on finding an effective control method of the CAVS and FingerVision-enabled hand for pivoting. We investigate the dynamic property of this system, develop some control methods, and empirically compare their performance. Through the experiments, we found that the timing when the grasped object starts rotating is unpredictable and the rotation speed rapidly increases after the start of rotation. We also found that CAVS reduces the rapid increase of rotation speed. Based on these findings, we introduced two control methods; one is a fuzzy control to decide the speed of fingertip opening with a simple rule set, and the other is a vibration control where a high frequent vibrating motion is added to the fingertip motion. In these controls, we used the orientation of the object estimated by FingerVision. The further empirical study demonstrated that the vibration control outperforms the fuzzy control. The experimental results also showed that the CAVS skin provides better control accuracy than a usual flat skin especially when the pivoting object is lightweight.

The rest of this paper is organized as follows. Section II discusses the related work. Section III describes our robot hand system. In Section IV, we investigate the dynamic property of this system. Section V introduces 2 control methods for pivoting. Section VI and VII show our experimental results and discussions. Section VIII concludes this paper.

II. RELATED WORK

A. Pivoting

There are decades of history in the research related to pivoting. Early studies were done by Carlisle et al. [4] and Rao et al. [5] where industrial parts were pivoted vertically around a grasped point in order to align the orientation of the parts efficiently in a product line of a factory. Dafle et al. introduced a concept of "extrinsic dexterity" to in-hand manipulation especially re-grasping [3], where they pointed out that in-hand manipulation performed by non-dexterous robot hands relies on resources extrinsic to the hand such as gravity, external contacts, and dynamic arm motions. There are some studies of pivoting with extrinsic dexterity. Holladay et al. [6] proposed a method of generating trajectories to transit between stable poses using the external contacts. In [7]–[9], dynamic arm motions were used to generate a pivoting motion using moment of inertia. Some studies introduced (deep) reinforcement learning to optimize such dynamic arm motions to achieve pivoting [10], [11]. While those work focused on the motions and control methods, our work explores the effectiveness of the finger surface structure (CAVS) in pivoting.

The pivoting task considered in this paper also relies on extrinsic dexterity, more specifically we use gravity to make a rotational motion of grasped objects. There are some studies of the similar approaches. Dafle et al. [12] created a gripper that can switch between a point contact and a multi-point contact depending on the grasping force; this gripper was able to align a grasped object upright by rotating around the point contact. Vina et al. [13] proposed a method to calculate the optimal grasp force for a desired trajectory from the contact and dynamics models of the soft fingers during pivoting, and maintain the force by feedback control with a force sensor. They also introduced a method of continuously updating the friction coefficient estimation model during pivoting an object; they explored the method with target objects made with various materials. Costanzo et al. [14] introduced a tactile sensor in pivoting control; the pose of a grasped object is observed through the tactile sensor, and is used to control the rotation speed of the object. Much of those work has focused on accurate contact and dynamic modeling to achieve the desired dynamic pivoting motion. In contrast, we explore how the CAVS skin contributes to pivoting compared to a usual flatskin of the fingertips. Our expectation is that the CAVS skin provides a gentle control during rotating the object because of the low-friction mode.

B. Variable friction

The main way to change the friction on the robot surface is to control the surface roughness and adhesion force. A method to change friction by changing surface wrinkles by tension, compression, UV, electricity [15]–[17], etc. has been proposed. In contrast, a method has been proposed to change the friction by changing the adhesion force with variable temperature, lubricant, electricity, and material [18]–[21].

However, it is not well understood what kind of object manipulation is facilitated by changing the friction on the

robot surface. Only a few studies have attempted to manipulate objects with a robot hand that has a variable friction surface. Spiers et al. [22] showed that it is easy to achieve in-hand rolling manipulation with high friction surface and in-hand sliding manipulation with low friction condition. Nojiri et al. [23] showed that when manipulating the tube, the firm holding of the tube can be obtained on a high-friction surface, while a change in contact position due to sliding can be easily obtained on a low-friction surface.

These manipulations are considered as static tasks, i.e. the robot hand and the objects do not move dynamically. It is still an open question how effective are the variable friction surfaces in dynamic manipulation tasks such as pivoting. We explore the pivoting task with CAVS in order to provide some insights to this question.

III. CAVS and FingerVision-Enabled Robot Hand

We introduce our robot hand equipped with CAVS (variable friction surface) and FingerVision (vision-based tactile sensor). Fig. 2 shows the entire system where the base robot hand is a two finger four DoF gripper driven by timing belts and four Dynamixel motors. FingerVision and CAVS are installed on the fingertips of the hand.

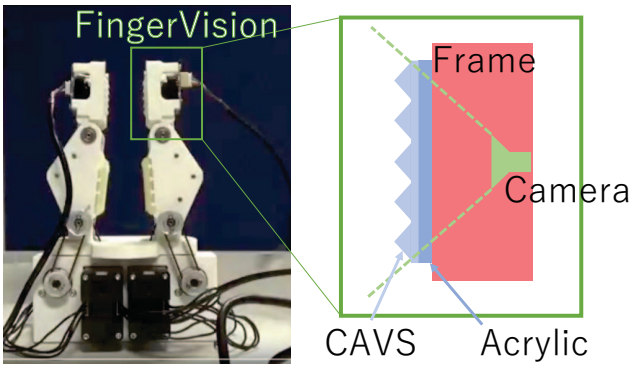

Fig. 2: CAVS and FingerVision-enabled robot hand

CAVS, the contact area variable surface, is a mechanism developed by Nojiri et al. [1] that is passively deformed by an external load, and the friction coefficient changes according to the contact area change. CAVS in this paper has flexible and hollow cone-shaped protrusions on its surface. The mechanism of the variable friction of CAVS is illustrated in Fig. 3. When a smaller force is applied, only the tips of the protrusions contact the object and the contact area is small. When a larger force is applied, the protrusions are pressed and deformed and thus the contact area is increased. In this way, the CAVS passively switches between a low-friction mode (smaller load, smaller contact area) and a high-friction mode (larger load, larger contact area) according to an external load. The low-friction mode will be good for manipulation using on-purpose slips, while the high-friction model is desirable to stable grasping.

FingerVision is a vision-based tactile sensor developed by Yamaguchi et al. [2], [24]. FingerVision consists of a transparent and flexible skin and a camera underneath, as shown

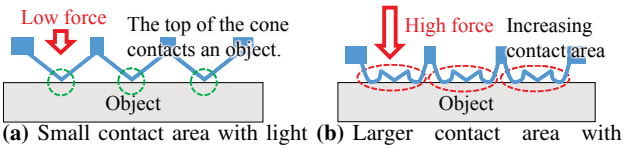

(a) Small contact area with light touch. **(b)** Larger contact area with heavier touch

Fig. 3: The protrusions of CAVS deform under load and the contact area is increased accordingly.

in Fig. 2. In the original version of FingerVision, markers are placed on the surface of the skin and the camera can track the markers according to the skin deformation, which provides an estimate of the external force distribution. In addition to that, the FingerVision camera can see through the skin (direct vision), which provides other modalities such as slippage and object shape, texture, and orientation. In order to combine FingerVision with CAVS, CAVS is made with a transparent material (Elastic resin from Formlabs co., shore hardness 50A) printed with the Form3 3D-printer. In our current implementation, the CAVS surface does not have markers, and we use only the direct vision in this paper. More specifically, we use the angle θ of a grasped object estimated from the FingerVision camera by an image processing.

IV. Experimental Analysis of CAVS Properties

We conduct preliminary experiments to investigate the dynamic properties of CAVS in a pivoting scenario compared with a normal flat-shape skin (FLAT) made with the same material as CAVS. Based on these results, we design an appropriate control for pivoting.

In order to investigate the fundamental properties of CAVS, we use a simple open-loop control. At the beginning of each trial, we let the robot hand grasp firmly an object at the horizontal position. Then we slowly and gradually increase the fingertip opening until it reaches to a target distance. During the whole trial, the orientation of the object is measured with FingerVision. The experiments are performed with CAVS and FLAT respectively, with varying target distances.

The expected results are as follows. With FLAT, the grasped object may suddenly start slipping at a certain fingertip opening because of the grasp force drop. This phenomenon can be avoided with CAVS. Initially CAVS works at the high-friction mode during grasping the object firmly, then it switches to the low-friction mode with the increase of the fingertip opening (i.e. decrease of the grasp force). At that time, the grasped object will start slipping, but that change will be more gradual than that with FLAT due to the low-friction mode. During the low-friction mode, the grasped object keeps rotating around the grasped point.

A. Results

The robot hand grasps the edge of an object (metal ruler, $16\,[\mathrm{g}]$) at the horizontal position ($0\,[\mathrm{deg}]$) and opens the fingertips at a constant speed of $0.5\,[\mathrm{mm/s}]$ until it reaches to a target distance. This trial is repeated by changing the target distance for CAVS and FLAT.

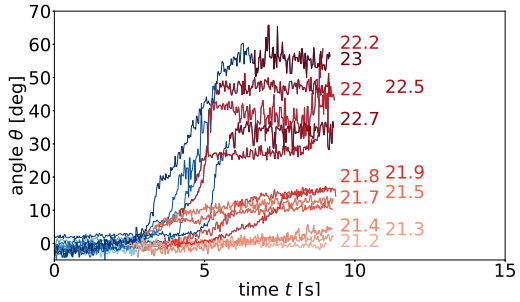

(a) CAVS

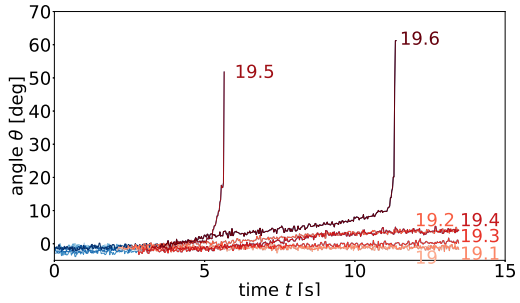

(b) FLAT

Fig. 4: Angle profiles in the simple pivoting with different target fingertip positions. The labels in the figure indicate the target positions.

The results are shown in Fig. 4. Individual curve shows an angle profile of the object per time for a target gripper position. Each curve has a blue and a red parts; the finger is moving during the blue part, while the finger is stopping during the red part after reaching to the target position. Each motion was terminated when the angle change was not observed for while or the robot dropped the object.

We can see two patterns in Fig. 4(b); one is keep holding the object around the initial angle, and the other is a sudden increase of the angle. In these experiments, we did not observe an intermediate change. On the other hand, Fig. 4(a) shows that the angle is gradually changing. With a larger target fingertip opening, the both angular velocity and reaching angle becomes gradually larger. We consider that this phenomenon is caused by the variable friction of CAVS as we hypothesized above. In the pivoting task, this property is desirable to the precise control.

Furthermore, we can find the following properties of this system: *Property (1)* The timing when the object starts rotating is hard to predict. Sometimes the object starts rotating during opening the fingertips, while it starts some seconds after the fingertip opening reaches at the target position, i.e. there is significant latency. This phenomenon can be found both in CAVS and FLAT. This phenomenon would be due to the elastic material of the skin, the CAVS structure, and the weight of the object (light). *Property (2)* Once if the object starts rotating, the increase of the angular speed is rapid. Although this increase of CAVS is (much) less than that of FLAT, the speed increase is still large. Furthermore, the variance of the speed increase is large, i.e. it is also hard to predict.

Both *Properties (1)* the significant and unpredictable latency and *(2)* unpredictable speed increase make it difficult to construct a dynamics model of the system. PD control is hard to handle it; adjusting the gain parameters is difficult especially due to *Property (2)*. We also cannot expect a good performance with model predictive control and differential dynamic programming due to the large variances of latency and state changes. Note that the reason why model-based control worked in past work such as [13], [14] would be that they used heavier objects which reduce those variances and make the dynamics tractable.

V. Control Methods for Pivoting

Based on the findings mentioned in Section IV, we design adequate control methods for pivoting with the CAVS and FingerVision-enabled robot hand. Since it seems that stabilizing the angular velocity of the object is difficult, we consider two approaches; fuzzy control and vibration control. Then, we introduce a termination process to stop the object at a target angle.

A. Fuzzy Control

The idea of introducing the fuzzy control is that since there are different dynamic modes in the system, making a different control policy for each mode seems to be adequate. We construct a simple rule set to form a fuzzy control: when the grasped object is not rotating (A), the gripper opening velocity is positive; when the angular velocity of the object is within a target range (B), the gripper velocity is zero; when the object is rotating too fast (C), the gripper velocity is negative. This approach was initially explored in our preliminary work [25]. More specifically, Table I shows the set of rules to decide he gripper opening velocity v according to the angular velocity $\dot{\theta}$ of the grasped object. This control policy is applied at each control cycle.

TABLE I: Opening and closing velocity of hand

Parameter	Condition A	Condition B	Condition C
Angular velocity $\dot{\theta}$	$\dot{\theta} < \dot{\theta}_{ltrg}$	$\dot{\theta}_{ltrg} \leq \dot{\theta} \leq \dot{\theta}_{utrg}$	$\dot{\theta}_{utrg} < \dot{\theta}$
Gripper velocity v	v_{open}	0	v_{close}

B. Vibration Control

Due to *Properties (1)* and *(2)*, updating the control command (fingertip opening position) after observing the change of angular velocity of the object would be too late to reduce the angular velocity. The vibrating motion introduced here enforces the fingertip closing motion regardless the angular velocity. Thus, we expect that the rapid increase of the angular velocity can be somehow decreased. Concretely, we consider a fingertip opening control like the fuzzy control as the baseline. Then we add a high frequent vibrating motion with a small amplitude to the fingertip opening.

Fig. 5 illustrates a trajectory of fingertip opening (gripper position) generated by the vibration control. It consists of a baseline motion and additional wave motions. The baseline

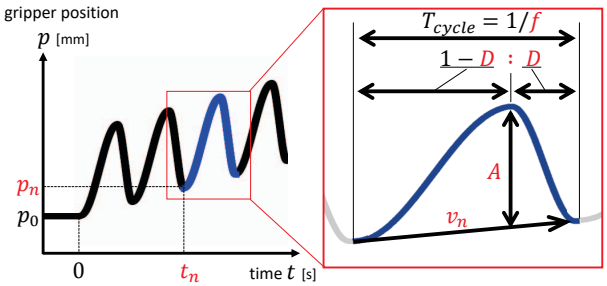

Fig. 5: A trajectory of fingertip opening (gripper position) generated by the vibration control

motion is defined by a recursive form. An n-th cycle starts with a gripper position p_n at time t_n, and during that cycle, it generates a linear motion with the constant velocity v_n. The period of each cycle is $1/f$ where f is the frequency of the cycles. Thus, the baseline motion is $p(t) = p_n + v_n(t - t_n)$ where $p(t)$ is the gripper position at time t ($t_n \leq t < t_{n+1}$), and $t_{n+1} = t_n + 1/f$, $p_{n+1} = p_n + v_n/f$.

An asymmetric wave motion is added to this baseline motion. Each wave starts at t_n and ends at t_{n+1}, i.e. it has the same cycle as the baseline motion. Each wave motion is based on a shifted upside-down cosine function with amplitude A, i.e. $\frac{A}{2}\{1-\cos 2\pi f(t-t_n)\}$, but it is deformed asymmetrically with the duty ratio $D \in [0, 1]$. D denotes the ratio of the closing and the opening periods in a wave. The rising part and the falling part have different velocities; when $D < 0.5$, the closing velocity is faster than that of opening velocity. The purpose of this asymmetric wave is to handle *Properties (1)* and *(2)* by closing faster the gripper. Thus, typically we use a smaller $D < 0.5$.

By adding this asymmetric wave motion to the baseline motion, we obtain the trajectory of the vibration control. The gripper position at time $t \in [t_n, t_{n+1})$ is given by the function P of Eq. 1.

$$P(t) = p_n + v_n(t - t_n) + \begin{cases} \frac{A}{2}\{1 - \cos\frac{2\pi f}{2(D-1)}(t - t_n)\} \\ \qquad t_n \leq t < t_n + \frac{(1-D)}{f} \\ \frac{A}{2}\{1 + \cos\frac{2\pi f}{2D}(t - t_n - \frac{(1-D)}{f})\} \\ \qquad t_n + \frac{(1-D)}{f} \leq t < t_n + \frac{1}{f} \end{cases} \quad (1)$$

The objective of the vibration control mentioned above is to handle *Properties (1)* and *(2)*. In addition to that, we apply a rule-based method to control the baseline motion so that we can obtain a desired pivoting motion. The idea is the same as the fuzzy control. Specifically, the gripper velocity v_n is chosen from $\{v_{open}, 0, v_{close}\}$ according to the angular velocity $\dot{\theta}$ of the grasped object. In contrast to the fuzzy control introduced in the last section, the rule set here is more complicated to work with the vibration control. The rules are as follows: if $\dot{\theta}$ is within $[0, \dot{\theta}_{trg}]$ during the last cycle ($t \in [t_n, t_{n+1})$), $v_{n+1} = v_{open}$; if $\dot{\theta}$ exceeds $\dot{\theta}_{trg}$ anytime during the last cycle and $\dot{\theta} \leq \dot{\theta}_{trg}$ at $t = t_{n+1}$, $v_{n+1} = 0$; if $\dot{\theta} > \dot{\theta}_{trg}$ at $t = t_{n+1}$, the vibration control is interrupted and a gripper closing motion is inserted until $\dot{\theta} \leq \dot{\theta}_{trg}$ is satisfied. In the gripper closing motion, the gripper velocity v_{close} is used. After the gripper closing motion, the vibration control is resumed with using the current gripper position as p_{n+1} and $v_{n+1} = v_{open}$. The entire algorithm is described in Algorithm 1 where dt denotes the control period ($1/120$ [s]).

Algorithm 1 Vibration control method

```
n ← 0
p_n ← p_0, v_n ← v_open, t_n ← 0
loop
  while t < t_n + 1/f do
    t ← t + dt
    Observe θ̇_t
    p ← P(t)
    Command the hand with p
  end while
  if θ̇_t > θ̇_trg then
    Execute the gripper closing motion with v_close
    v_{n+1} ← v_open
  else if max_{t'∈[t_n, t_n+1/f)} θ̇_{t'} ≥ θ̇_trg then
    v_{n+1} ← 0
  else
    v_{n+1} ← v_open
  end if
  p_{n+1} ← p, t_{n+1} ← t
  n ← n + 1
end loop
```

C. Termination Process

Finally, we design a termination process to stop the grasped object at a target angle. Note that the pivoting manipulation of this paper is irreversible, so we can not kick back the object when it exceeds the target angle. We approximate the recent object angle sequence with a quadratic form, and estimate the duration to reach the target angle with it. If this duration is smaller than a threshold, we close the hand immediately to firmly grasp the object. In the experiments, we use 0.1 [s] as this threshold, which was empirically decided with considering the delays of the system. The modeling of the object angle sequence and the termination time estimation are done at each control cycle.

Due to *Properties (1)* and *(2)*, the estimation of the termination time is sometimes inaccurate. If the difference between the object angle and the target is more than a threshold, we repeat the control until the difference becomes smaller than the threshold or the object angle goes beyond the target. This threshold should be decided according to the minimum angle that the pivoting control can rotate the object. We conducted a preliminary experiment to choose this value, and chose 3 [deg].

VI. Experiments

We conduct experiments of pivoting with the robot system described in Section III. FingerVision sensor provides the angle θ and the angular velocity $\dot{\theta}$ of the grasped object

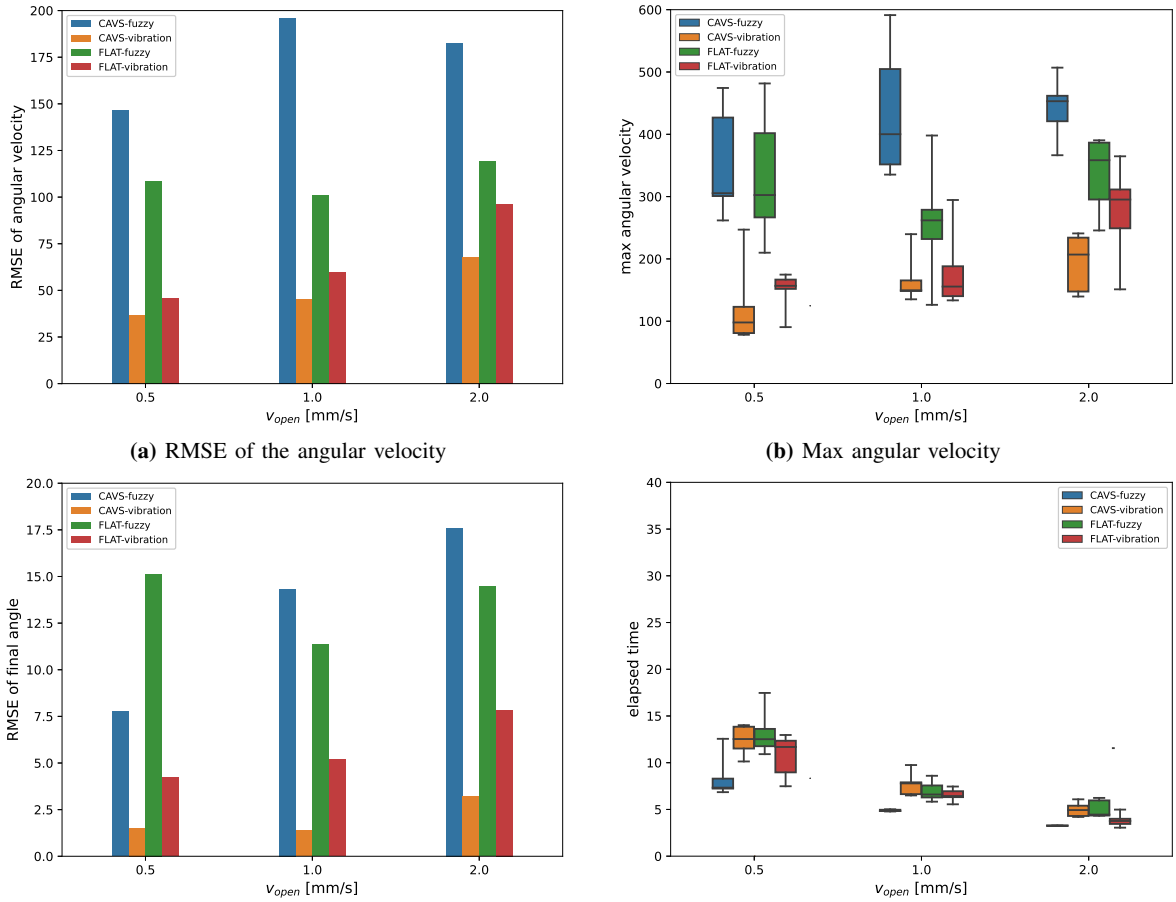

(a) RMSE of the angular velocity

(b) Max angular velocity

(c) RMSE of the final angle

(d) Elapsed time

Fig. 6: Results of pivoting the metal ruler.

at 60 [Hz]. We operate the gripper position p on position control at 120 [Hz]. Thus, we use 120 [Hz] as the control loop frequency where the FingerVision signals are temporality filtered.

The pivoting task is performed as follows; first, we let the hand grasp the edge of an object at the horizontal pose (0 [deg]), then rotate the object to $\theta_{trg} = 60$ [deg] using a control method described in Section V.

Table II shows the control parameters used in the experiments. In addition to them, we configured the parameter of the vibration control to be $\dot{\theta}_{trg} = 15$ [deg/s] and the parameters of the fuzzy control to be $\dot{\theta}_{ltrg}, \dot{\theta}_{utrg} = 10, 15$ [deg/s]. They are decided by experimental trial and error.

TABLE II: Control parameters used in the experiments

Method	f [Hz]	A [mm]	D [−]	v [mm/s]	
				v_{open}	v_{close}
Vibration	5	3	0.1	0.5, 1, 2	−2.0
Fuzzy	-	-	-	0.5, 1, 2	−2.0

We compare all four combinations of CAVS or FLAT as the finger surface, and the fuzzy or the vibration control as the control method. Each combination is tested with two kinds of objects, a metal ruler and a wood block, that have different mass and moment of inertia as shown in Table III. Furthermore, in each case, we test three different v_{open} values 0.5, 1, 2 [mm/s]. Thus, we have 24 conditions in total. Each condition is performed five times to acquire a statistical data.

TABLE III: Moment of inertia and mass of the objects used in the experiments

Object	I [kg $*$ cm^2]	m [g]
Metal ruler	0.93	16
Wood block	3.77	80

In order to evaluate the performance of each condition from several aspects, we use the following four indices. All indices are computed from the five trials.

1) **RMSE of the angular velocity**
   Root mean square error between the angular velocity of the object $\dot{\theta}$ and the target $\dot{\theta}_{trg}$ or $\dot{\theta}_{utrg}$ only if $\dot{\theta} > \dot{\theta}_{trg}$ or $\dot{\theta} > \dot{\theta}_{utrg}$.
2) **Max angular velocity**
   Maximum value of $\dot{\theta}$ during the operation.
3) **RMSE of the final angle**
   Root mean square error between the final object angle θ and the target angle θ_{trg}.
4) **Elapsed time**
   Duration of the control.

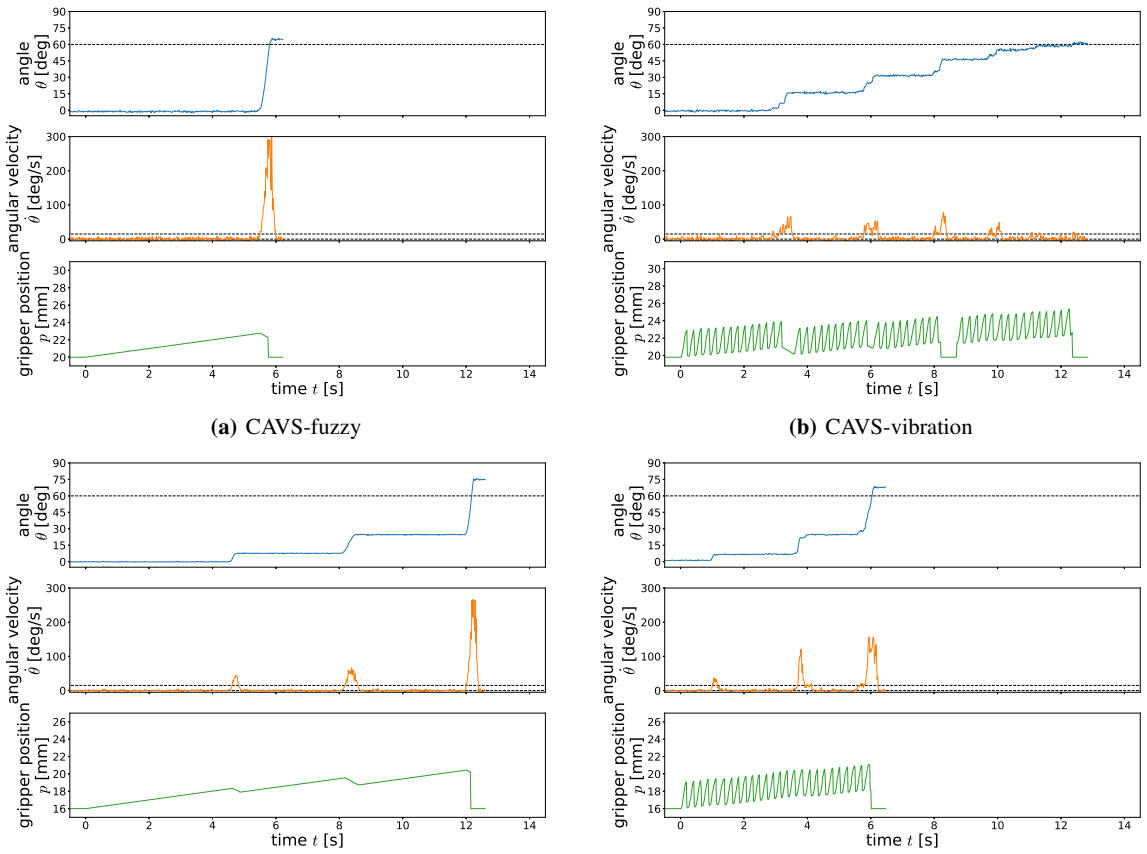

(a) CAVS-fuzzy

(b) CAVS-vibration

(c) FLAT-fuzzy

(d) FLAT-vibration

Fig. 7: Pivoting the metal ruler; an example of time series graph during pivoting at $v_{open} = 0.5\,[\mathrm{mm/s}]$. Each shows under combinations of CAVS or FLAT as the finger surface, and the fuzzy or the vibration control as the control method. Each horizontal axis is on the same scale. Data was not sampled after pivoting was completed.

Both the RMSE of the angular velocity and the max angular velocity show how much the sudden increase of the angular velocity of the object is reduced (smaller values are preferable). RMSE of the final angle shows the control accuracy of pivoting (smaller values have higher accuracies). Elapsed time shows the cost of control time.

A. Pivoting a Lightweight Metal Ruler

Fig. 6 shows the results of four indices in 12 conditions of pivoting the metal ruler. From the RMSE of the angular velocity and the max angular velocity graphs(Fig. 6(a), 6(b)), we can find that the conditions with the fuzzy control have larger values, i.e. the angular velocities were not controlled well. Among them, those of CAVS is larger than those of FLAT, which means that this control method is not adequate for CAVS to exploit its capability found in the preliminary experiments. However the vibration control reduced those values effectively, and in this case, the values of CAVS are smallest for all v_{open}. These results seem to be explaining the difference of control accuracies in the RMSE of the final angle graph(Fig. 6(c)). The vibration control with CAVS condition has the smallest RMSE for each v_{open}, i.e. it is the most accurate. Note that the reason why the RMSE increases according to v_{open} is that the smaller gripper velocity is better for the control accuracy. The best accuracy is 2 degree, which was achieved with CAVS and the vibration control at $v_{open} = 0.5\,[\mathrm{mm/s}]$. From the elapsed time graph(Fig. 6(d)), we can see that a larger v_{open} reduces the control duration. Thus, there is a trade-off between the RMSE of the final angle and the elapsed time, and v_{open} can deal with the trade-off.

Fig. 7 shows an example of time series graph of the object angle, angular velocities and gripper position during pivoting. In CAVS-fuzzy(Fig. 7(a)), the execution time is small since the target angle was achieved at once by a sudden and rapid increase of angular velocity. In CAVS-vibration(Fig. 7(b)), we can see that the angular velocity is much smaller. With this small angular velocity, the object angle reached close to the target angle. At $t = 8\,[\mathrm{s}]$, the termination process was activated, but the pivoting was resumed because the remaining error of the angle was larger than the threshold. In FLAT-fuzzy(Fig. 7(c)) and FLAT-vibration(Fig. 7(d)), we can see a similar trend between the different control methods. However it seems that the angular velocities of FLAT-vibration are larger than those of CAVS-vibration. This is due to the CAVS structure.

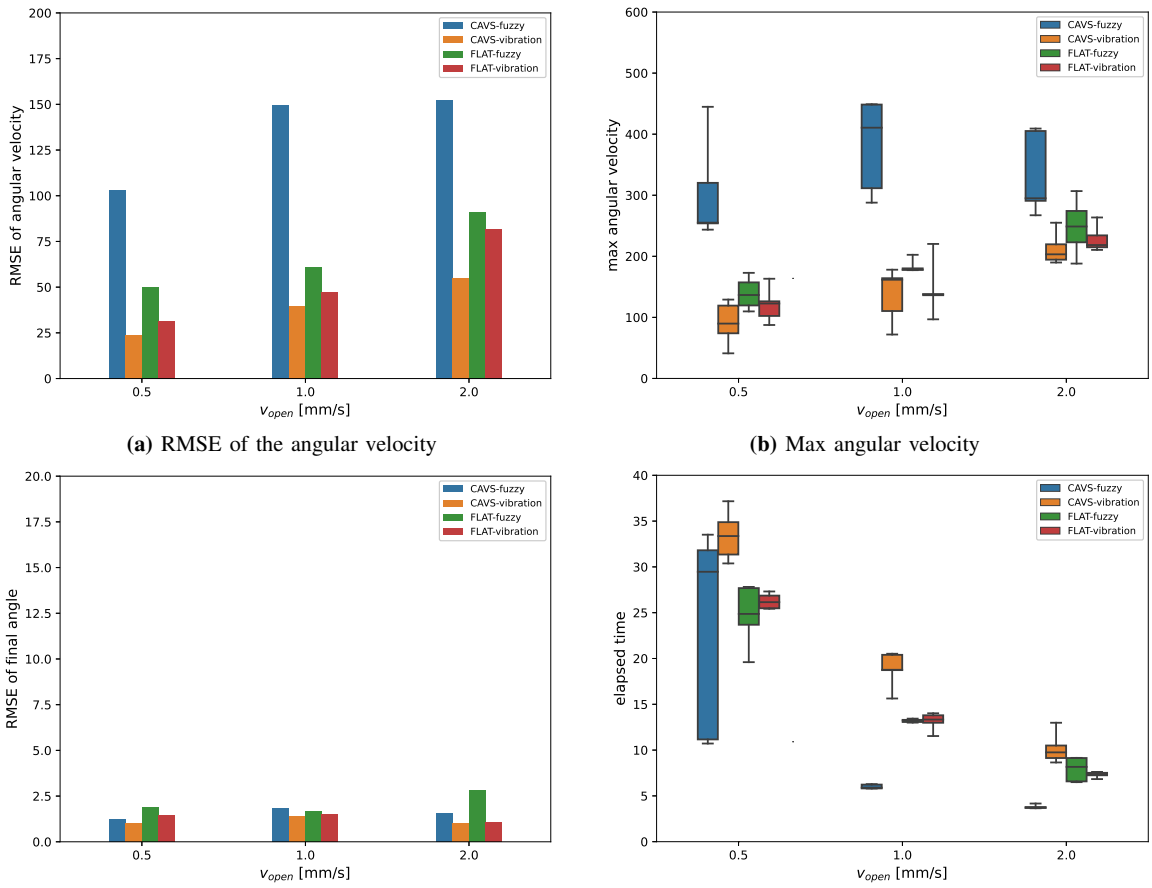

(a) RMSE of the angular velocity

(b) Max angular velocity

(c) RMSE of the final angle

(d) Elapsed time

Fig. 8: Results of pivoting the wood block.

B. Pivoting a Wood Block

Fig. 8 shows the results of four indices in 12 conditions of pivoting the wood block. From the RMSE of the angular velocity, the max angular velocity, and the RMSE of the final angle graphs(Fig. 8(a), 8(b), 8(c)), we can see the similar trend as that of pivoting the metal ruler. Namely, CAVS with the vibration control works effectively. However, the control error was within about 2 degree for all conditions, regardless of the control method or surface. This would be due to the weight of the object; heavier objects may be easier for stable pivoting. Comparing the elapsed time between Figs. 6(d) (the metal ruler cases) and 8(d) (the wood block cases), we can see the time of the ruler is shorter than that of the wood block. It means that the object is moving more slowly in the wood block cases, which might have caused the good accuracy.

VII. Discussion

In all cases of pivoting with the CAVS skin and the vibration control, we obtained a good accuracy, i.e. the RMSEs of the final angles were lowest. This means that the CAVS skin with the vibration control is able to handle *Properties (1)* and *(2)* mentioned in Section IV. Especially in the pivoting of the metal ruler, the CAVS skin with the vibration control outperformed the other conditions.

From the results of the metal ruler cases and the wood block cases, we can say that the inertial characteristics of the objects affects the pivoting dynamics and the control performance. When the objects are lightweight like the ruler, *Properties (1)* and *(2)*, i.e. the unpredictability of rotation start timing and the rapid rotational speed increase, become stronger. Due to that, we can clearly see the differences of the four conditions (CAVS+fuzzy, CAVS+vibration, FLAT+fuzzy, FLAT+vibration) in the pivoting of the ruler. We discuss further about these cases in the following.

Why the vibration control improves the accuracy? Comparing the results in the different control pairs (CAVS+fuzzy vs. CAVS+vibration, FLAT+fuzzy vs. FLAT+vibration), using the vibration control is better in accuracy. This means that our hypothesis, the rapid increase of the angular velocity can be decreased since the vibrating motion enforces the closing motion, is correct.

Why CAVS with the vibration control is the best? During the rotation in pivoting, the object slips on the fingertips. The friction force between the object and the fingertips should be small enough to slip, while the larger friction force is desirable to avoid a too rapid slippage. Although a further analysis is necessary, we think that the low friction mode of CAVS contributes in this situation. Since the friction force is proportional to the load (and the load is proportional to the fingertip opening) where the proportionality constant is the friction coefficient, the lower friction coefficient of the CAVS

in the low friction mode provides more accurate control. Thus, CAVS+vibration outperformed FLAT+vibration.

Why CAVS with the fuzzy control is not good? Comparing CAVS+fuzzy and FLAT+fuzzy, we do not see a performance improvement with CAVS. We think this is due to the rapid rotational speed increase and the response of the CAVS skin. In the fuzzy control, the robot starts closing the fingertips when it observes a too large rotational speed. Since CAVS is in the low friction mode, it needs to move more than FLAT to have enough friction force to stop the rotation. This slower response might have caused the bad performance of CAVS+fuzzy.

VIII. Conclusion

In this paper, we explored effective control methods for the CAVS and FingerVision-enabled robot hand through a pivoting task. CAVS is a skin for robots where the surface friction coefficient passively changes according to the external force, and we expected that CAVS provides a gentle control in in-hand manipulation. FingerVision is a vision-based tactile sensor that can be installed under a variety of robotic skins due to the flexibility. In our study, FingerVision is embedded under CAVS and the observed signals are used in manipulation. The pivoting task in this paper uses gravity to make a slip to rotate the object, where we expected that the low friction mode of CAVS improves the control accuracy. However a proper control scheme was unclear to achieve this.

We designed two control methods, a fuzzy control and a vibration control, through the preliminary experiments, and conducted further experiments to compare the performance differences in the pivoting task. We compared the CAVS and FLAT skins, those two control methods, and two objects (lightweight and heavier) to be pivoted. The results demonstrated that the CAVS skin with the vibration control outperforms the other methods. Especially in pivoting the lightweight object, the other methods showed performance drops while the CAVS with the vibration control presented a good control accuracy.

Acknowledgment

Yamaguchi was supported in part by the Canon Foundation 10th Research Grant Program (K18-0105).

References

[1] S. Nojiri, K. Mizushima, Y. Suzuki, T. Tsuji, and T. Watanabe, "Development of contact area variable surface for manipulation requiring sliding," in *IEEE International Conference on Soft Robotics*, 2019, pp. 131–136.

[2] A. Yamaguchi and C. G. Atkeson, "Tactile behaviors with the vision-based tactile sensor fingervision," *International Journal of Humanoid Robotics*, vol. 16, no. 03, p. 1940002, 2019.

[3] N. C. Dafle, A. Rodriguez, R. Paolini, B. Tang, S. S. Srinivasa, M. Erdmann, M. T. Mason, I. Lundberg, H. Staab, and T. Fuhlbrigge, "Extrinsic dexterity: In-hand manipulation with external forces," in *2014 IEEE International Conference on Robotics and Automation (ICRA)*. IEEE, 2014, pp. 1578–1585.

[4] B. Carlisle, K. Goldberg, A. Rao, and J. Wiegley, "A pivoting gripper for feeding industrial parts," in *Proceedings of the 1994 IEEE International Conference on Robotics and Automation*. IEEE, 1994, pp. 1650–1655.

[5] A. Rao, D. J. Kriegman, and K. Y. Goldberg, "Complete algorithms for feeding polyhedral parts using pivot grasps," *IEEE Transactions on Robotics and Automation*, vol. 12, no. 2, pp. 331–342, 1996.

[6] A. Holladay, R. Paolini, and M. T. Mason, "A general framework for open-loop pivoting," in *2015 IEEE International Conference on Robotics and Automation (ICRA)*. IEEE, 2015, pp. 3675–3681.

[7] A. Sintov and A. Shapiro, "Swing-up regrasping algorithm using energy control," in *2016 IEEE International Conference on Robotics and Automation (ICRA)*. IEEE, 2016, pp. 4888–4893.

[8] J. Shi, J. Z. Woodruff, P. B. Umbanhowar, and K. M. Lynch, "Dynamic in-hand sliding manipulation," *IEEE Transactions on Robotics*, vol. 33, no. 4, pp. 778–795, 2017.

[9] S. Cruciani and C. Smith, "In-hand manipulation using three-stages open loop pivoting," in *2017 IEEE/RSJ International Conference on Intelligent Robots and Systems (IROS)*. IEEE, 2017, pp. 1244–1251.

[10] R. Antonova, S. Cruciani, C. Smith, and D. Kragic, "Reinforcement learning for pivoting task," *arXiv preprint arXiv:1703.00472*, 2017.

[11] S. Stepputtis, Y. Yang, and H. B. Amor, "Extrinsic dexterity through active slip control using deep predictive models," in *2018 IEEE International Conference on Robotics and Automation (ICRA)*. IEEE, 2018, pp. 3180–3185.

[12] N. Chavan-Dafle, M. T. Mason, H. Staab, G. Rossano, and A. Rodriguez, "A two-phase gripper to reorient and grasp," in *2015 IEEE International Conference on Automation Science and Engineering (CASE)*. IEEE, 2015, pp. 1249–1255.

[13] F. E. Vina B., Y. Karayiannidis, C. Smith, and D. Kragic, "Adaptive control for pivoting with visual and tactile feedback," in *2016 IEEE International Conference on Robotics and Automation (ICRA)*, 2016, pp. 399–406.

[14] M. Costanzo, G. De Maria, and C. Natale, "Control of sliding velocity in robotic object pivoting based on tactile sensing," *IFAC-PapersOnLine*, vol. 53, no. 2, pp. 9950–9955, 2020.

[15] K. Suzuki and T. Ohzono, "Wrinkles on a textile-embedded elastomer surface with highly variable friction," *Soft Matter*, vol. 12, no. 29, pp. 6176–6183, 2016.

[16] D. Liu and D. J. Broer, "Self-assembled dynamic 3d fingerprints in liquid-crystal coatings towards controllable friction and adhesion," *Angewandte Chemie International Edition*, vol. 53, no. 18, pp. 4542–4546, 2014.

[17] H. Abdi, M. Asgari, and S. Nahavandi, "Active surface shaping for artificial skins," in *2011 IEEE International Conference on Systems, Man, and Cybernetics*. IEEE, 2011, pp. 2910–2915.

[18] S. Kim, M. Sitti, T. Xie, and X. Xiao, "Reversible dry micro-fibrillar adhesives with thermally controllable adhesion," *Soft Matter*, vol. 5, no. 19, pp. 3689–3693, 2009.

[19] K. Mizushima, Y. Suzuki, T. Tsuji, and T. Watanabe, "Deformable fingertip with a friction reduction system based on lubricating effect for smooth operation under both dry and wet conditions," *Advanced Robotics*, vol. 33, no. 10, pp. 508–519, 2019.

[20] J. Shintake, S. Rosset, B. Schubert, D. Floreano, and H. Shea, "Versatile soft grippers with intrinsic electroadhesion based on multifunctional polymer actuators," *Advanced materials*, vol. 28, no. 2, pp. 231–238, 2016.

[21] K. P. Becker, N. W. Bartlett, M. J. Malley, P. M. Kjeer, and R. J. Wood, "Tunable friction through constrained inflation of an elastomeric membrane," in *2017 IEEE International Conference on Robotics and Automation (ICRA)*. IEEE, 2017, pp. 4352–4357.

[22] A. J. Spiers, B. Calli, and A. M. Dollar, "Variable-friction finger surfaces to enable within-hand manipulation via gripping and sliding," *IEEE Robotics and Automation Letters*, vol. 3, no. 4, pp. 4116–4123, 2018.

[23] S. Nojiri, A. Yamaguchi, Y. Suzuki, T. Tsuji, and T. Watanabe, "Sensing and control of friction mode for contact area variable surfaces (friction-variable surface structure)," in *3rd IEEE International Conference on Soft Robotics, RoboSoft 2020*. Institute of Electrical and Electronics Engineers Inc., 2020, pp. 215–222.

[24] A. Yamaguchi and C. G. Atkeson, "Combining finger vision and optical tactile sensing: Reducing and handling errors while cutting vegetables," in *2016 IEEE-RAS 16th International Conference on Humanoid Robots (Humanoids)*. IEEE, 2016, pp. 1045–1051.

[25] Y. Suzuki, A. Yamaguchi, S. Nojiri, T. Watanabe, and K. Hashimoto, "In-hand manipulation by a robot hand equipped with friction-variable surface and vision-based tactile sensor," in *Proceedings of the 2021 JSME Conference on Robotics and Mechatronics*, 2021, [in Japanese].